Impact of the *Aqua* MODIS Band 6 Restoration on Cloud/Snow Discrimination

IRINA GLADKOVA, FAZLUL SHAHRIAR, AND MICHAEL GROSSBERG

NOAA/CREST, City College of the City University of New York, New York, New York

RICHARD A. FREY AND W. PAUL MENZEL

Cooperative Institute for Meteorological Satellite Studies, Madison, Wisconsin

(Manuscript received 20 March 2013, in final form 28 August 2013)

ABSTRACT

Distinguishing between clouds and snow is an intrinsically challenging problem because both have similar high albedo across many bands. The 1.6-μm channel (band 6) on the Moderate Resolution Imaging Spectroradiometer (MODIS) instrument provides an essential tool for distinguishing clouds from snow, since snow typically has a much lower albedo in this band. Unfortunately, this band is severely damaged on the MODIS/*Aqua* platform and is typically not used in either snow or cloud products. An algorithm was previously introduced for quantitative image restoration (QIR) that can restore missing pixels of band 6 using multilinear regression with input from a spatial-spectral window in other bands. Also previously demonstrated was the effectiveness of this restoration for snow products over cloud-free pixels only. The focus of the authors' previous work was to evaluate the impact of this restoration on the snow product, and they had relied on the current cloud mask, which does not use any information from band 6. In this work the authors propose to apply the QIR-corrected band 6 to directly create a new cloud mask. They demonstrate that this new cloud mask is much more consistent with the one produced using the undamaged MODIS band 6 on *Terra*. The restoration of MODIS band 6 on the *Aqua* platform and its impact on the discrimination of clouds, snow, and clear sky is also examined. A comprehensive evaluation was conducted on a global set of granules. The method shows great promise and should be considered for use in NASA's next reprocessing of *Aqua* MODIS data.

1. Introduction

Snow and clouds are often very challenging to distinguish, since they frequently have matching reflectance across many spectral bands. In the visible portion of the spectrum, clouds and snow are nearly equally highly reflective. In the infrared portion, low stratus clouds show very little thermal contrast when compared to snow-covered ground. Thin cirrus are also difficult to separate from surface snow using thermal infrared channels, as much of the radiation from the surface is transmitted through the cloud. Spectral bands from the near-infrared part of the spectrum, such as 1.6 μm, are often crucial for distinguishing cloud and snow, since snow is less reflective in that band when compared with clouds. Thus, the cloud, snow, and ice identification developed by the National Aeronautics and Space Administration (NASA) for the Moderate Resolution Imaging Spectroradiometer (MODIS) incorporated observations in MODIS band 6, which is centered at 1.6 μm.

The 1.6-μm measurements from band 6 of MODIS on the *Terra* platform are used in both the cloud and snow products. The corresponding band 6 data from the instrument on the *Aqua* platform is not directly usable for this purpose, however, because of the failure of many of its detectors (see Salomonson and Appel 2006). As a result, *Aqua* MODIS snow and cloud products have been forced to use MODIS band 7 centered at 2.1 μm instead of the preferable band 6 (see Hall et al. 2002; Riggs and Hall 2004). Although using band 7 produces reasonable results for snow products, they are thought to be inferior to results produced using the fully functioning band 6 (see Hall and Riggs 2007). It is important to note that some of the MODIS *Aqua* band 6 detectors are still functioning; this enables a quantitative image restoration (QIR) of MODIS *Aqua* band 6 data as described in Gladkova et al. (2012c). This restoration is based on the fact that

Corresponding author address: Irina Gladkova, NOAA/CREST, City College of the City University of New York, 160 Convent Avenue, New York, NY 10031.
E-mail: gladkova@cs.ccny.cuny.edu

DOI: 10.1175/JTECH-D-13-00066.1

© 2013 American Meteorological Society

the other spectral bands on multispectral imagers often contain enough information to accurately estimate the missing spectral band data. While individual channels may not share strong enough pairwise correlation with the missing band, nonlinear multivariate relationships can be exploited to recover the missing pixel values.

In previous work (Gladkova et al. 2012b,a), we showed that the restoration was effective at producing a snow mask from *Aqua* of comparable quality to that from *Terra* for pixels that were cloud free. In that work we relied on the current *Aqua* cloud mask, which does not use band 6, despite the fact that we had restored it. This is particularly a problem in cases of nearly complete surface snow cover and partial cloud cover. The 1.6-μm channel is particularly useful for distinguishing snow from cloud, but since the prior work did not modify the cloud mask, it would not show any improvement in this case, where a restored 1.6-μm channel could have the greatest impact.

In this paper we argue for using our restored band 6 for the cloud mask as well. We show that when using the restored band 6 of *Aqua* MODIS, the resulting cloud mask agrees more closely with the *Terra* MODIS cloud mask than the currently used approach involving band 7 instead of band 6. We show the impact on discrimination between clouds, snow, and clear sky after the band 6 restoration on *Aqua* MODIS by applying the same algorithm used for *Terra* MODIS. We compare the result based on the restored band 6 with that of band 7. We also perform a test of QIR on band 6 of *Terra* MODIS (artificially degrading band 6 in simulation of that on *Aqua*) and compare the resulting *Terra* snow mask with the original. To account for a wide variety of conditions and terrains, we conducted a comprehensive evaluation on a global day's worth of *Terra* MODIS granules (157 granules in total).

2. Snow and cloud determination

Clouds are generally characterized by higher reflectance and lower temperature than the underlying the earth's surface. Simple visible and infrared window threshold approaches offer considerable skill in cloud detection; however, there are many surface conditions when this characterization of clouds is inadequate, most notably over snow and ice. The 36-channel MODIS offers the opportunity for multispectral approaches to cloud detection, so that discriminating between snow- and ice-covered surfaces and clouds may be better accomplished.

In daytime scenes, MODIS band 4 and 6 reflectances (0.55 and 1.6 μm, respectively) are combined in a normalized difference to detect snow and ice on the earth's surface (Hall et al. 1995), the normalized difference snow index (NDSI), defined as $\mathrm{NDSI} = (R_{0.55} - R_{1.6})/(R_{0.55} + R_{1.6})$. Snow and ice surfaces are characterized by high values of reflectivity in band 4 but very low values in band 6, leading to $\mathrm{NDSI} \gg 0$. On the other hand, water phase clouds are very reflective at both wavelengths, generating NDSI values close to 0. The cloud mask makes use of this measure along with other spectral tests to discriminate between clouds and snow/ice on the surface. The method was successfully incorporated into the MODIS *Terra* cloud mask (MOD35) but was severely compromised for MODIS *Aqua* because of a majority of band 6 detectors being either nonfunctional or extremely noisy. Band 7 (2.1 μm) was substituted for band 6 and is used in the *Aqua* cloud mask with a different snow/ice versus cloud threshold ($\mathrm{NDSI} > 0.75$ for *Aqua* vs $\mathrm{NDSI} > 0.4$ for *Terra*). Though band 7 reflectances are generally smaller than those of band 6, they are, in a relative sense, smaller compared to band 6 over clouds than over snow and ice. This makes NDSI with use of band 7 a less sensitive discriminator of snow/ice versus cloud than NDSI with use of band 6.

a. *Example with* Terra *MODIS data*

We present a case study of the use of the QIR algorithm for a cloud mask in the presence of snow. In this case study, all pixels happen to be either cloud or snow pixels. For evaluation purposes we have degraded a *Terra* MODIS granule over the Arctic from 16 April 2012 to match the damage present on an *Aqua* granule. To simulate the *Aqua*-like damage to the MODIS instrument on the *Terra* platform, we note that each of the MODIS detectors produces a specific scan line within a swath of data in each band. Most of band 6 *Aqua*/MODIS detectors are unusable, meaning that their data are missing or are very noisy (Salomonson and Appel 2006; Wang et al. 2006; Rakwatin et al. 2009). The list of broken detectors is well known and recorded by NASA in the file metadata. It can also be easily determined from inspection of the level 1 digital counts, since they either produce near-constant or near normally distributed noise values along the scan line. While it is possible that there is some residual useful information in some of the detectors, the QIR algorithm produces a high-quality restoration excluding these broken detector scan lines. Thus, the simulation of *Aqua* band 6 is accomplished by taking the values from a *Terra* granule and setting band 6 radiance values to a constant invalid value along the scan lines corresponding to those broken in the *Aqua*-based instrument. Since the QIR algorithm ignores these scan lines, the choice of invalid value is not important.

Our evaluation compares a generated cloud/snow product using the original unaltered data using band 6

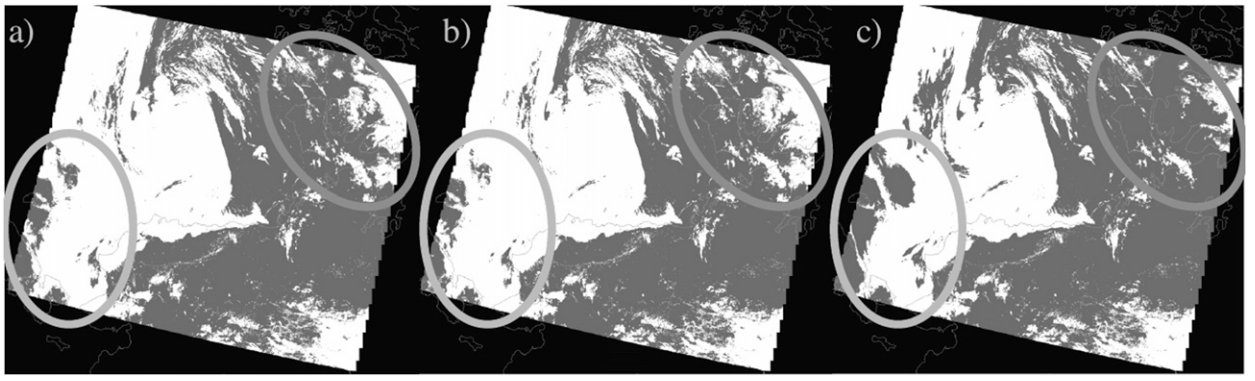

FIG. 1. MODIS *Terra* imagery and resulting cloud mask results at 2150 12 Apr 2012 UTC: (a) *Terra* snow mask (gray is snow) using original band 6 reflectances, (b) *Terra* snow mask using the QIR band 6, and (c) *Terra* snow mask using band 7 reflectances instead of band 6.

(Fig. 1a); the QIR-created cloud/snow mask based on *Aqua* MODIS–simulated damage to a *Terra* MODIS band 6 (Fig. 1b); and the substitute cloud/snow mask (Fig. 1c), where band 7 is used instead of band 6. The band 7 algorithm is borrowed from the current *Aqua* MODIS cloud/snow mask, but the thresholds have been adjusted to indicate the 10% higher reflectance in *Terra* band 7 compared to *Aqua* band 7. It is apparent after inspection of the cloud/snow masks that the QIR band 6 product (Fig. 1b) is closer to the original (Fig. 1a) than the substitute band 7 product (Fig. 1c). The QIR band 6 product finds a little less snow (Fig. 1b, red circle) than

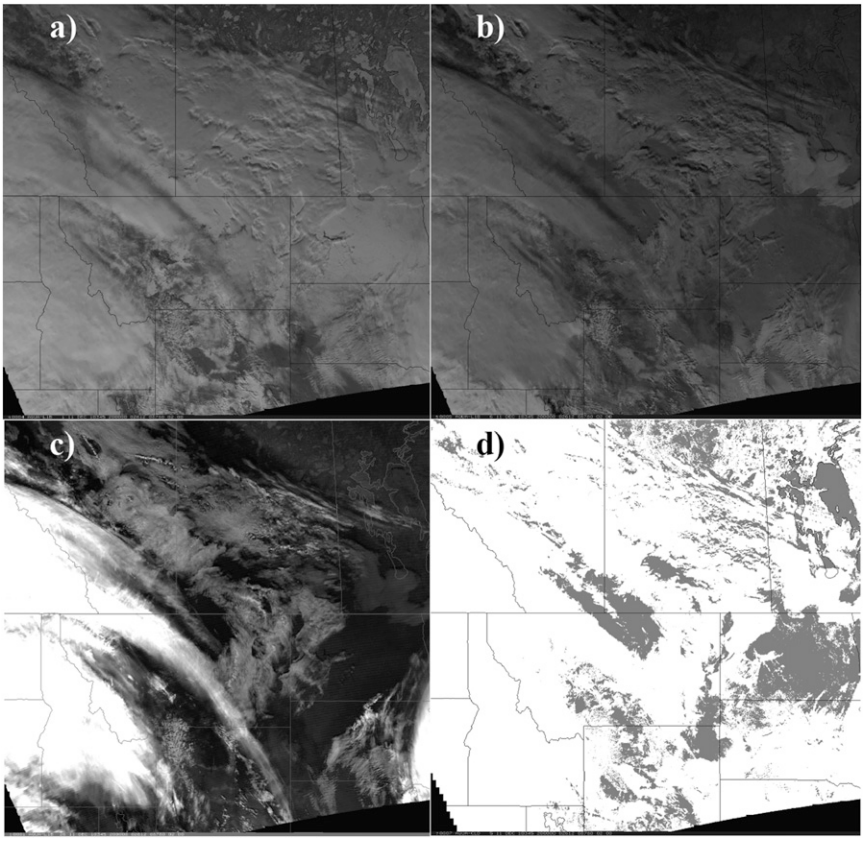

FIG. 2. MODIS imagery and resulting cloud mask results at 2000 UTC 11 Dec 2010: (a) *Aqua* MODIS band 4 (0.55 μm) image, (b) the QIR-corrected *Aqua* MODIS band 6 (1.6 μm) image, (c) *Aqua* MODIS band 26 (1.38 μm) image, and (d) original (collection 5 MOD35) *Aqua* snow detection image, where gray indicates snow and white cloud.

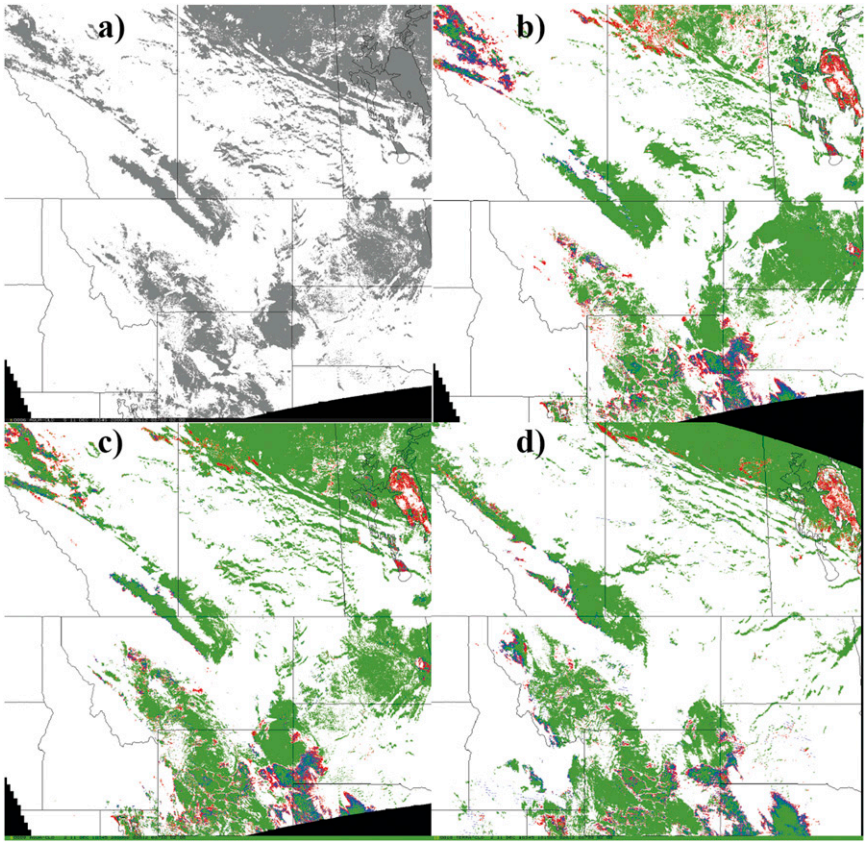

FIG. 3. MODIS imagery and resulting cloud mask results at 2000 UTC 11 Dec 2010: (a) the QIR-corrected *Aqua* snow detection image, (b) current operational *Aqua* cloud mask result (green is for confident clear, blue is for probably clear, red is for probably cloudy, and white is for cloud), (c) the QIR-corrected *Aqua* cloud mask result, and (d) *Terra* cloud mask result at 1815 UTC 11 Dec 2010. Note the area around Lake Winnipeg in the top-right corner of the images.

the original snow mask (Fig. 1a, red circle), but the result matches the original product much more than the substitute band 7 product (Fig. 1c, red circle). Also, the substitute band 7 product finds more snow incorrectly over thin cirrus (Fig. 1c, blue circle). Note that the difficulty in the discrimination of cirrus cloud and snow is highlighted in Miller et al. (2005). It is also important to note that the snow mask used in prior work (Gladkova et al. 2012b,a) assumed a clear-sky value for the snow identification and the cloud product did not use any of the band 6 data. Nearly all of the change in snow in this case study is due to changes in the determination of which pixels are classified as cloudy as a result of using the QIR-corrected band 6 for the cloud mask.

b. Example with Aqua *MODIS data*

Figures 2 and 3 show an *Aqua* MODIS scene from southwestern Canada and northwestern United States at 2000 UTC 11 December 2010. Snow and lake ice are clearly evident in the band 4 image (Fig. 2a) as well as in the QIR band 6 image (Fig. 2b), where water clouds (brighter) and snow/ice surface (darker) are contrasted. Figure 2c shows 1.38-μm imagery that is most sensitive to high cloud, where brighter cirrus clouds are very prominent. Figures 2d and 3a show results of the original (Fig. 2d) and the QIR (Fig. 3a) *Aqua* snow detection algorithm. The only changes made to the algorithm from the original were the decrease in the NDSI threshold noted above and a change to an absolute NIR reflectance threshold (from 2.1 to 1.6 μm). The increased sensitivity of the NDSI using the QIR-corrected band 6 reflectances is manifested as an increase in snow detected in the boreal forest region north and west of Lake Winnipeg (in the top-right corner of the image). On the other hand, the Great Plains region to the south of Lake Winnipeg shows less snow detected using the QIR band 6 rather than band 7 data. Figures 3b and 3c show the current operational cloud mask based on band 7 (Fig. 3b)

TABLE 1. Confusion matrix between the original and the QIR-corrected MOD35 on global data. Top values in each box are the number of pixels, and bottom values (parentheses) are the percentage of the total pixels. Global data from 28 Aug 2006. There are 369 435 808 pixels in total, out of which only 0.087% are off diagonal, showing excellent agreement with the reference data.

	QIR-corrected MOD35			
Original MOD35	Confident clear	Probably clear	Probably cloudy	Confident cloudy
Confident clear	89 783 064 (24.303)	921 (0.000)	2576 (0.001)	250 187 (0.068)
Probably clear	309 (0.000)	27 051 829 (7.322)	195 (0.000)	11 199 (0.003)
Probably cloudy	1099 (0.000)	143 (0.000)	13 362 182 (3.617)	19 977 (0.005)
Confident cloudy	33 357 (0.009)	1728 (0.000)	4507 (0.001)	238 912 454 (64.670)

and the QIR band 6 (Fig. 3c) cloud mask results. By definition, an accurate positive snow/ice decision by spectral testing excludes cloud cover; therefore, regions that have more accurate snow detection also have more accurate cloud detection. Finally, Fig. 3d shows the earlier *Terra* MODIS cloud mask from 1815 UTC 11 December 2010. There appears to be better agreement between *Terra* and *Aqua* cloud masks (especially in the region around Lake Winnipeg) when *Aqua* is using the QIR-corrected band 6, allowing for the roughly 2-h time difference in image acquisition. While this example is encouraging, global routine application of the QIR1.6-μm data would require careful tuning of the snow detection algorithm and the associated thresholds to accommodate the reflectance values in that reconstructed spectral band.

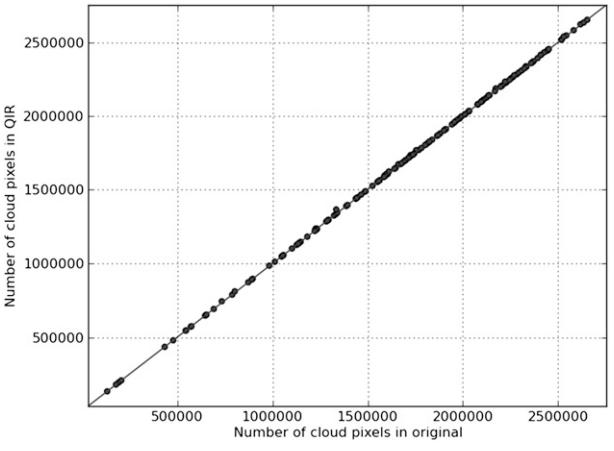

FIG. 4. The number of cloud pixels for each granule is shown. Each dot represents one granule, and the line is diagonal to the axes. We see that the number of cloud pixels is not overestimated or underestimated by a significant amount.

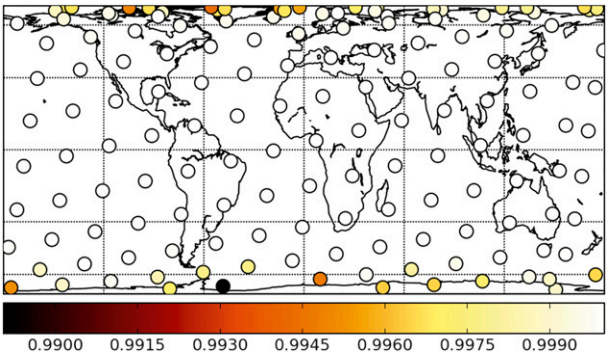

FIG. 5. Map showing accuracy for granules over a global day. Each circle is geolocated at the approximate center of the granule. The color bar indicates the accuracy over each granule. The primary problem for cloud discrimination is snow, which explains the high accuracy away from the poles. Part of Antarctica lacks errors since it is polar night (missing data), whereas in other parts, errors are high because of low light.

3. Performance of the QIR: One-day global

We evaluated the QIR-based cloud mask on a global dataset for 28 August 2006. Our evaluation is based on using *Terra* granules degraded to simulate band 6 damage on *Aqua*, as described in the previous section. We processed daytime granules only because band 6 has no effect on the cloud or snow mask at night. We focus on the performance of the algorithm in the Arctic under brighter sunlight, where the cloud mask algorithm using the original data performs better than in the lower-lighting conditions of the Southern Hemisphere.

The QIR algorithm restores band 6 in its native resolution of 500 m. However, the cloud mask algorithm is applied at 1-km resolution. Thus, we aggregated band 6 to 1 km, so it can be used to obtain the cloud mask. The confusion matrix containing the number of false

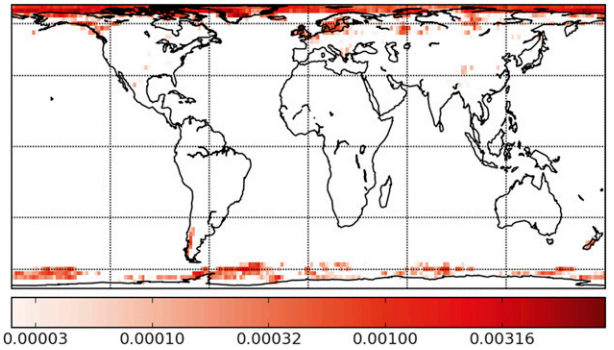

FIG. 6. Map showing density of false negative identification of cloud pixels per square kilomter over the global day. The bins were chosen using an equal-area projection. Note that false negatives (clouds identified as nonclouds) occur mostly near the Arctic and particularly in Greenland.

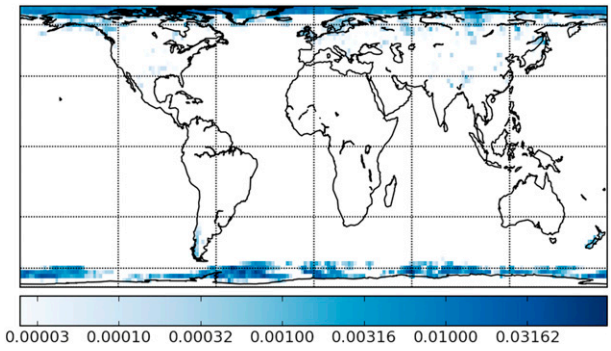

FIG. 7. Map showing density of false positive identification of cloud pixels per square kilometer over the global day. The bins were chosen using an equal-area projection. Note that false positives (nonclouds identified as clouds) occur mostly in low-light conditions near the Antarctic.

TABLE 2. Confusion matrix between original and the QIR-corrected MOD35 restricted to latitudes where snow is plausible. Top values in each box are the number of pixels, and bottom values (parentheses) are the percentage of the total pixels. Data are from 60° to 90°N on 28 Aug 2006. There are 75 364 806 pixels in total, out of which 0.206% are off diagonal, still showing excellent agreement with reference data.

	QIR-corrected MOD35			
Original MOD35	Confident clear	Probably clear	Probably cloudy	Confident cloudy
Confident clear	14 679 037 (19.477)	832 (0.001)	2377 (0.003)	122 874 (0.163)
Probably clear	318 (0.000)	1 756 525 (2.331)	159 (0.000)	5800 (0.008)
Probably cloudy	903 (0.001)	73 (0.000)	2 086 357 (2.768)	13 654 (0.018)
Confident cloudy	28 666 (0.038)	1494 (0.002)	4213 (0.006)	56 661 524 (75.183)

positives, false negatives, true positives, and true negatives for this global study is represented in Table 1. As seen in Table 1, the original and the QIR-corrected *Terra* cloud mask mostly agree. Only 0.087% of the pixels are in the off-diagonal entries of the table. Most of these off-diagonal entries come from a flip from confident clear in the original mask to a confident cloudy in the QIR-based mask (false positive); a smaller number comes from confident cloudy in the original to becoming confident clear in the QIR (false negative). This shows that the QIR-based mask tends to overestimate the number of cloud pixels in some cases. Screening using an over-aggressive cloud mask, which excludes too many cloudy pixels, is often more desirable than the opposite, which introduces cloud contamination. The total number of cloudy pixels in the QIR-based mask strongly agrees with the total number of cloudy pixels in the original mask as

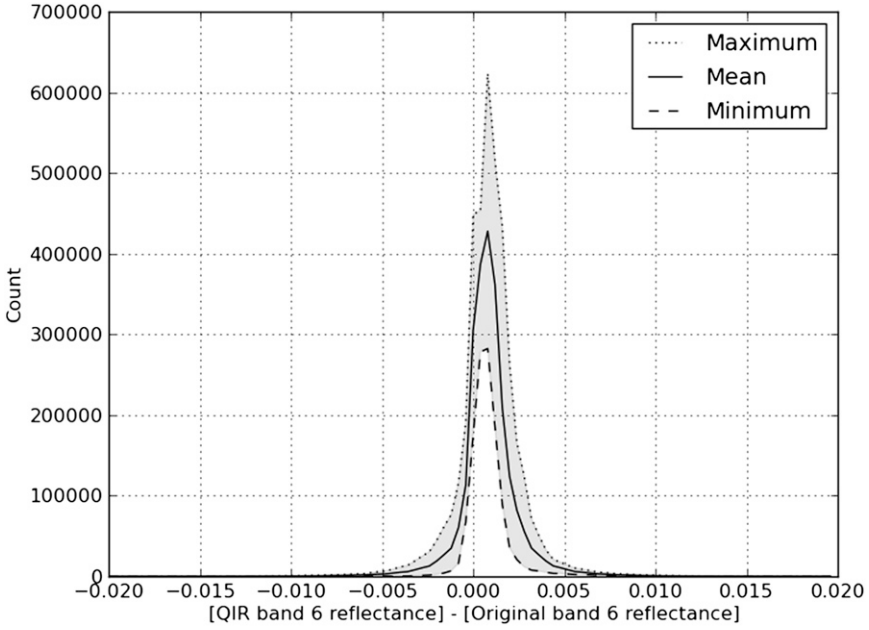

FIG. 8. Envelope derived from the histogram of reflectance value errors for each of the six granules. The granules were chosen over the polar regions, where cloud/snow discrimination is particularly challenging. The curves show the maximum, minimum, and mean count for a bin at a given error level (*x* axis) over the six granules. The shaded region represents the range of bin counts for that error level. Note that errors are generally stable and have small positive bias.

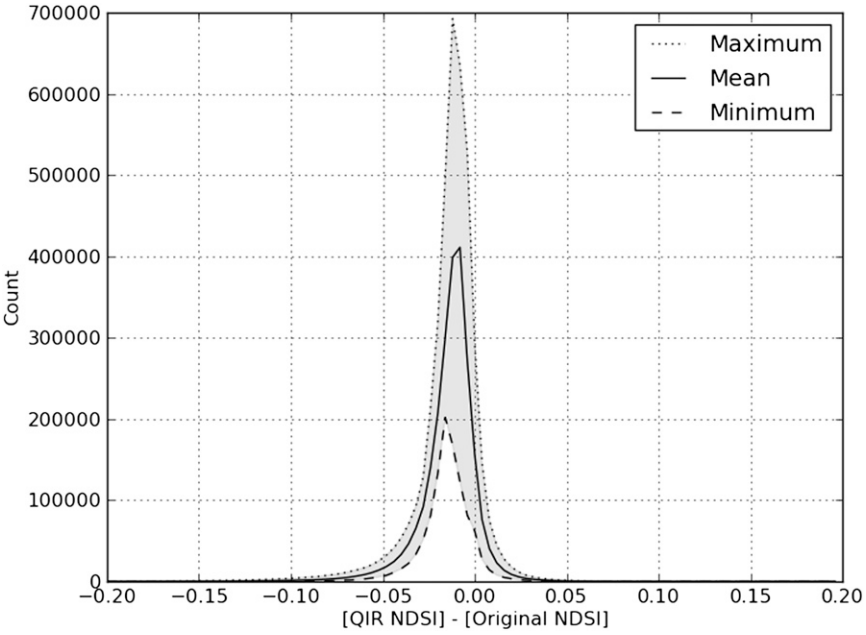

FIG. 9. Envelope derived from the histogram of NDSI errors for each of the six granules used in the previous figure. As in the previous figure, the curves show the maximum, minimum, and mean count for a bin at the error level, with the shaded region showing the range. Note here that the NDSI errors have a small negative bias, which may result in a small over detection of cloud.

shown in Fig. 4. There is no bias in the total number of cloudy pixels detected by the QIR, but the spatial distribution of the false detections is not uniform.

The geographic locations of granules and their accuracy are shown in Fig. 5. Most of the errors are occurring in the polar regions. Figures 6 and 7 display the geographic locations of the pixels with false negative (Fig. 6) and false positive (Fig. 7) cloud classification. The color pallet corresponds to the accuracy values for the corresponding granule, defined as

$$\text{Accuracy} = \frac{(\text{Number of true positives}) + (\text{Number of true negatives})}{(\text{Total number of classified pixels})}.$$

We have chosen the accuracy values for visualization, since it represents the proportion of true results (both true positives and true negatives) of the total and is indicative of classifier performance. As with the per granule evaluation, most of the errors appear near the poles. As can be seen from these figures, there are more false positive pixels (Fig. 7) than false negative pixels (Fig. 6), and they are sometimes concentrated around coastal regions (e.g., Greenland). We also see this in the confusion matrix for the higher latitudes (cf. Table 2). In the counts restricted to the data from 60° to 90°N, there are more (0.206%) misclassified pixels. Overall, the performance is quite good even in the most challenging regions. The accuracy values are very high, and the number of misclassifications is well less than 1%.

In investigating the six granules with the poorest performance (all in the polar regions), we find that there are no particular cloud types more likely than others to be changed by the QIR process. The pixels where disagreement is found have band 6 reflectances that are near clear/cloudy or snow/no-snow threshold values. Therefore, these pixels may be in either a cloudy or clear region, but as we see in the statistics, more pixels change from clear to cloudy than from cloudy to clear. The reason for this can be seen easily when comparing original and the QIR-corrected band 6 imagery—the QIR-corrected granules appear to have slightly higher reflectances than in the originals. The histogram of errors in the reflectance values for these six granules over the polar regions is shown in Fig. 8. The cumulative histogram of NDSI errors for the six granules over polar regions is shown in Fig. 9. As seen in Fig. 9, the NDSI computed with the QIR-based reflectances has slightly smaller values compared to the

original NDSI values. In general, this leads to less snow and more cloud determinations.

4. Conclusions

In this work we have shown that the QIR applied to band 6 on *Aqua* MODIS produces results that should be suitable for producing a cloud mask of comparable quality to the *Terra* MODIS product. The *Aqua* MODIS cloud mask generally detects more snow with use of the QIR band 6 (1.6 μm) than with band 7 (2.1 μm) for cloud or snow pixels because it recognizes more pixels as cloud free in agreement with similar results on *Terra*. In addition, it brings the *Aqua* cloud mask more into agreement with the earlier *Terra* cloud mask, thus diurnal changes in cloud, snow, and clear sky can be detected more reliably using the same algorithm.

We evaluated the QIR for the cloud mask using *Terra* MODIS (where band 6 is artificially degraded to simulate the *Aqua* band 6) and showed that the QIR band 6 cloud mask is preferable to a substitute band 7 mask when compared with the original *Terra* cloud mask from a case study over the polar region. It was noted that using the QIR-corrected band 6 versus band 7 yielded somewhat better discrimination between thin cirrus clouds and surface ice in this case. It is possible that other methods that preferentially use band 6 (but must substitute band 7 on *Aqua*) to separate cirrus clouds from snow and surface ice, such as Miller et al. (2005), may also benefit from using the QIR-corrected band 6. We evaluated a case study where we show that the QIR *Aqua* data produces a cloud mask that is more similar to the *Terra* cloud mask acquired a short time earlier.

In addition, we collected statistics on a global day of *Terra* data and showed statistically good agreement of the cloud mask using the QIR-corrected band 6 to the original cloud mask. As a result, we are confident that the QIR shows great promise and should be tested for incorporation into NASA's next collection (reprocessing) of *Aqua* MODIS data to provide complete and consistent cloud and snow products.

Acknowledgments. This work was supported in part by the NOAA/NESDIS STAR, Grant DG133E07CQ0077.

REFERENCES

Gladkova, I., M. Grossberg, G. Bonev, P. Romanov, G. Riggs, and D. Hall, 2012a: A full snow season in Yellowstone: A database of restored Aqua band 6. *IEEE Geosci. Remote Sens. Lett.,* **10,** 553–557.

——, ——, ——, ——, and F. Shahriar, 2012b: Increasing the accuracy of MODIS/Aqua snow product using quantitative image restoration technique. *IEEE Geosci. Remote Sens. Lett.,* **9,** 740–743.

——, ——, F. Shahriar, G. Bonev, and P. Romanov, 2012c: Quantitative restoration for MODIS band 6 on Aqua. *IEEE Trans. Geosci. Remote Sens.,* **50,** 2409–2416.

Hall, D., and G. Riggs, 2007: Accuracy assessment of the MODIS snow products. *Hydrol. Processes,* **21,** 1534–1547.

——, ——, and V. Salomonson, 1995: Development of methods for mapping global snow cover using Moderate Resolution Imaging Spectroradiometer (MODIS) data. *Remote Sens. Environ.,* **54,** 127–140.

——, ——, ——, N. DiGirolamo, and K. J. Bayr, 2002: MODIS snow-cover products. *Remote Sens. Environ.,* **83,** 181–194.

Miller, S., T. Lee, and R. Fennimore, 2005: Satellite-based imagery techniques for daytime cloud/snow delineation from MODIS. *J. Appl. Meteor.,* **44,** 987–997.

Rakwatin, P., W. Takeuchi, and Y. Yasuoka, 2009: Restoration of Aqua MODIS band 6 using histogram matching and local least squares fitting. *IEEE Trans. Geosci. Remote Sens.,* **47,** 613–627.

Riggs, G., and D. Hall, 2004: Snow mapping with the MODIS Aqua instrument. *Proc. 61st Eastern Snow Conf.,* Portland, ME, ESC, 81–84.

Salomonson, V. V., and I. Appel, 2006: Development of the Aqua MODIS NDSI fractional snow cover algorithm and validation results. *IEEE Trans. Geosci. Remote Sens.,* **44,** 1747–1756.

Wang, L. L., J. J. Qu, X. Siong, H. Xianjun, X. Yong, and C. Nianzeng, 2006: A new method for retrieving band 6 of Aqua MODIS. *IEEE Geosci. Remote Sens. Lett.,* **3,** 267–270.